Equilibrium Data and Thermodynamic Modeling of Nitrogen, Oxygen, and Air Clathrate Hydrates

Amir H. Mohammadi, Bahman Tohidi,* and Rod W. Burgass

Center for Gas Hydrate Research, Institute of Petroleum Engineering, Heriot-Watt University, Edinburgh EH14 4AS, Scotland, U.K.

Air hydrates can form at high-pressure and low-temperature conditions found in deep ice sheets of Arctic and Antarctic regions. These hydrates can play a major role in analyzing the data gathered in these regions. However, there are limited experimental data and thermodynamic modeling on air hydrates. In this work, we present new experimental data on methane, nitrogen, oxygen, and air hydrates. An experimental setup based on a quartz crystal microbalance (QCM) has been used in measuring all the experimental data reported in this work. The QCM method needs much smaller samples, resulting in a significant reduction in the time required for each experiment. The available data on oxygen hydrates are used in optimizing the Kihara potential parameters for oxygen hydrates. Using the previously reported nitrogen Kihara potential parameters and the optimized Kihara potential parameters for oxygen, the hydrate stability zone of air hydrates (21 mol % oxygen and 79 mol % nitrogen) has been predicted. The predictions of the thermodynamic model are in good agreement with the independent experimental data on air hydrates, demonstrating the reliability of experimental and modeling techniques used in this work.

Introduction

Gas hydrates are solid crystalline compounds stabilized by the inclusion of suitably sized gas molecules inside cavities, of different sizes, formed by water molecules through hydrogen bonding. They resemble ice in appearance, but unlike ice, they may form at temperatures well above the ice point. Gas hydrates have been reviewed in depth by Sloan.[1]

Air hydrates are found in Arctic and Antarctic ice sheets, where air trapped during snowfalls becomes stable hydrates at high-depth and low-temperature conditions. The air and/or air hydrates trapped in ice sheets could provide valuable information on the atmospheric conditions at the time of the snowfall (i.e., thousands of years ago). Another potential application of hydrates is in solving the mysteries of Lake Vostok in Antarctic.[2] Lake Vostok is unique, as it is the largest lake buried beneath some four kilometers of ice. Ice core samples taken close to the surface of the lake have been dated as 420 000 years old, suggesting that the lake has been sealed beneath the ice cap for between 500 000 and in excess of one million years. The lake is arguably one of the most unique environments in the world, particularly as it may contain living organisms isolated from the rest of the world for over a million years. It is argued that the role of air hydrates should be taken into account in solving the mysteries of Lake Vostok. In addition, reliable experimental data and predictive models in the hydrate−ice−gas (HIG) and hydrate−liquid water−gas (HLG) regions are vital in simulating various past and future climate changes.

Experimental data on nitrogen, oxygen, and air hydrates are necessary for developing and validating predictive methods. Kuhs et al.[3] have reported three points in the hydrate−ice−gas (HIG) region for air hydrates. There seems to be no experimental data for air hydrates in the hydrate−liquid water−gas (HLG) region. Experimental data for nitrogen hydrates have been measured by van Cleeff and Diepen,[4,5] Marshal et al.,[6] Jhaveri and Robinson,[7] Miller[8] (one point in the HIG region), and Kuhs et al.[3] (four points in the HIG region). Van Cleeff and Diepen[4,5] have reported a good set of experimental data for oxygen hydrates. Kuhs et al.[3] have also presented two points in the HIG region for oxygen hydrates.

A number of correlations have been presented to calculate the stability zones for nitrogen, oxygen, and air hydrates. Miller[8,9] presented expressions for the decomposition conditions of nitrogen, oxygen, and air hydrates, which have frequently been cited in the literature. Lipenkov and Istomin[10] and Kuhs et al.[3] have presented an empirical correlation for nitrogen, oxygen, and air hydrates, using three different sets of constants.

All previous measurements are based on conventional experimental techniques, using visual or graphical techniques. Tohidi et al.[11] have reported a novel technique for measuring the hydrate stability zone based on the change in the resonant frequency of a quartz crystal microbalance (QCM). The authors reported significant reductions in the sample size and the time requirement as two major benefits of their new technique.

In this work, the QCM technique has been used in generating the experimental data. First, a set of hydrate dissociation points has been measured on methane and nitrogen hydrates to examine the reliability of the new technique and the experimental setup against literature data. Then the setup has been used in measuring data on oxygen and air hydrates. The available data on oxygen hydrates have been used in optimizing the Kihara potential parameters for oxygen and the extension of the existing thermodynamic model to this gas. Finally, the predictions of the thermodynamic model have been compared with the measured experimental data on air hydrates, demonstrating the reliability of the thermodynamic model.

* Corresponding author. Telephone: +44 (0)131 451 3672. Fax: +44 (0)131 451 3127. E-mail: Bahman.Tohidi@pet.hw.ac.uk.

10.1021/je025608x CCC: $25.00
Published on Web 03/26/2003

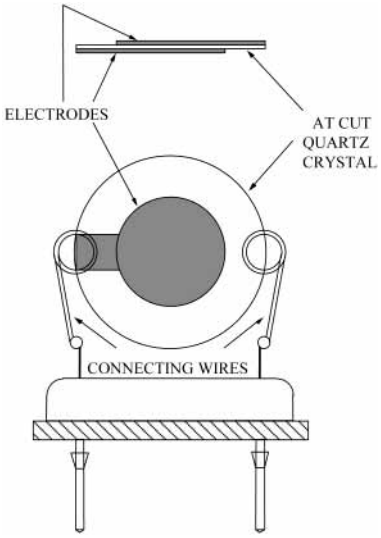

Figure 1. Schematic illustration of the QCM.

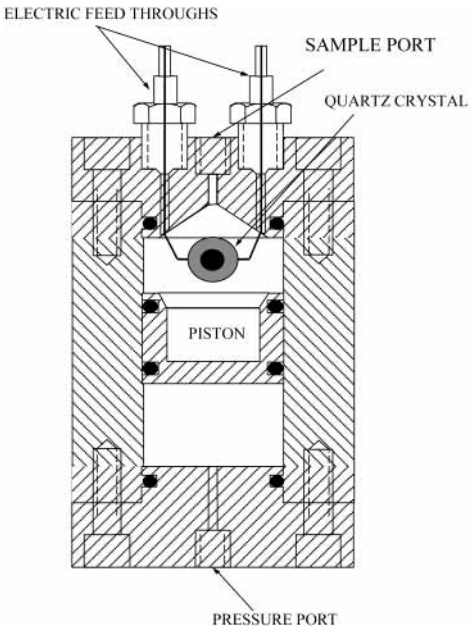

Figure 2. Schematic illustration of the QCM mounted within a high-pressure cell.

Experimental Equipment and Technique

A detailed description of the experimental setup and test procedures is given elsewhere.[11] The quartz crystal microbalance (QCM) was initially developed for the measurement of small changes in mass, hence the term "microbalance". It is extremely sensitive; a 1 ng mass change will result in a 1 Hz frequency change. The mass change can easily be determined from the frequency response by the Sauerbrey relationship.[12] The QCM has since proven to be a useful sensor in a wide variety of applications.[13−15] In this application the sensitivity of the QCM is utilized to determine the presence and absence of gas hydrates.

The crystals used in the data presented here were 5 MHz unpolished. Figure 1 is a diagram of the QCM. In the measurements presented here an HP 4194A impedance/gain-phase analyzer was used. The impedance analyzer is used to measure the resonant frequency of the crystal and its conductance at resonant frequency. Both of these electrical parameters can be used in conducting the measurements, as shown in the results. The crystal was mounted in a 150 cm^3 variable volume stainless steel cell as shown in Figure 2. The cell was surrounded by a water jacket in order to control the temperature.

The method employed in the tests presented here was that a drop of water was placed on one surface of the quartz crystal. The cell temperature was then lowered below 0 °C in order to freeze the water. The cell was then evacuated and the test fluids were introduced into the cell. The cell temperature and pressure were then adjusted to give conditions favorable for hydrate formation. The formation of hydrates was obvious through significant reductions in the resonant frequency and conductance at resonant frequency of the quartz crystal. The cell temperature was then raised stepwise, and the pressure and electrical parameters of the QCM were recorded at each step. The amount of water used was too small to give any significant drop in pressure on the formation of gas hydrates. As only a small amount of hydrates was formed, the time taken to dissociate them was also short, enabling the temperature to be stepped up rapidly, at around 15 min per temperature step (compared to several hours in a conventional cell) for the results presented in this work.

Four sets of hydrate dissociation data are presented here for methane, nitrogen, oxygen, and air hydrates with ±0.2 K and ±34.47 kPa uncertainty in the temperature and pressure measurements, respectively. Table 1 shows the purity and supplier of the test gases used.

Table 1. Compositions and Suppliers of the Test Gases Used in This Work

gas	purity (%)	supplier
methane	99.995	Air Products Ltd.
nitrogen	99.998	BOC Ltd.
oxygen	99.999	BOC Ltd.
air	18−21 mol % oxygen (zero grade)	Air Products Ltd.

Thermodynamic Modeling

A general phase equilibrium model based on uniformity of the fugacity of each component throughout all the phases[16,17] was extended to model the equilibrium conditions of nitrogen and oxygen (hence air) hydrates. A single equation of state (EoS), namely, the Valderrama[18] modification of the Patel and Teja equation of state (VPT EoS) with non-density-dependent mixing rules,[19] was used to determine component fugacities in all fluid phases. The fugacity of ice was rigorously calculated by correcting the saturation fugacity of water at the same temperature by an exponential factor (the Poynting correction). The hydrate phase was modeled by the solid solution theory of van der Waals and Platteeuw,[20] as developed by Parrish and Prausnitz.[21] For hydrate phases, the Kihara[22] potential parameters with a spherical core were selected to describe the potential function of all the molecules forming the hydrate phases. Also, for the heat capacity difference between the empty hydrate lattice and the pure liquid water, the equation recommended by Holder et al.[23] was used. Table 2 shows thermodynamic reference properties for hydrates used in this model.

The structure of nitrogen and oxygen hydrates is the subject of some debates. Before experimental determination of hydrate structures, it was assumed that nitrogen and oxygen formed structure I hydrates. Davidson et al.[25] determined that nitrogen and oxygen form structure II gas hydrates using low-temperature neutron and X-ray diffraction. Structure II of oxygen hydrates also has been examined by Tse et al.[26] with powder neutron diffraction

Table 2. Thermodynamic Reference Properties for Structure I Hydrates

	sI	ref
$\Delta\mu^{\circ}_{w}$/(J mol^{-1})	1297	24
Δh°_{w}/(J mol^{-1})[a]	1389	24
Δv_{w}/(cm^3 mol^{-1})[b]	3.0	21
ΔC°_{pw}/(J mol^{-1}K^{-1})[c]	−37.32	23
b/(J mol^{-1} K^{-2})[c]	0.179	23

[a] In the liquid water region subtract 6009.5 J mol^{-1} from Δh°_{w}. [b] In the liquid water region add 1.601 cm^3 mol^{-1} to Δv_{w}. [c] Values to be used in $\Delta C_{pw} = \Delta C^{\circ}_{pw} + b(T - T_0)$.

Table 3. Measured Methane Hydrate Dissociation Conditions in the HLG Region

T/K ± 0.2	P/kPa ± 34.47
278.85	4729.76

Table 4. Measured Nitrogen Hydrate Dissociation Conditions in the HLG Region

T/K ± 0.2	P/kPa ± 34.47
274.55	19 093.21
277.55	25 379.5
283.05	45 355

at very low-temperature conditions. Tohidi-Kalorazi[27] and Hendriks et al.[28] noticed that assuming structure I hydrates for nitrogen at ambient conditions gives a better agreement with the experimental nitrogen hydrate dissociation data than assuming structure II hydrates. However, their model showed that nitrogen changes to structure II hydrates at very low-temperature conditions.

The optimization of the Kihara potential parameters showed that nitrogen and oxygen are likely to form structure I gas hydrates under the conditions investigated in this work and structure II hydrates at very low temperatures, which is in agreement with that reported by Tohidi-Kalorazi[27] and Hendriks et al.[28] Therefore, the crystal structure of nitrogen and also oxygen is assumed to be structure I under the temperature conditions investigated in this work.

There is also some disagreement on the crystal structure of air hydrates. Miller,[8] who proposed the natural occurrence of air hydrates in deep Antarctic ice for the first time, assumed structure I for hydrates. Recently, Hondoh et al.[29] have shown that air hydrates have structure II at 255 K using X-ray diffraction. In this work, the hydrate stability zones of air hydrates, assuming structures I and II, have been calculated and compared with the experimental data. The results showed that structure I hydrates are in good agreement with the experimental data. Furthermore, the model predicts structure II for air hydrates at 255 K, as measured experimentally by Hondoh et al.[29]

Results and Discussions

Initially, hydrate dissociation conditions for methane and nitrogen hydrates were measured and compared with the literature data. Tables 3 and 4 present the experimental data measured in this work. Figure 3 shows the good agreement between nitrogen experimental data measured in this work and those reported in the literature.

Kihara potential parameters and thermodynamic modeling have been reported for nitrogen by several authors.[1,27] Using our previously reported Kihara potential parameters and assuming structure I hydrates under normal conditions, the hydrate stability zone of nitrogen hydrates is calculated and plotted in Figure 3.

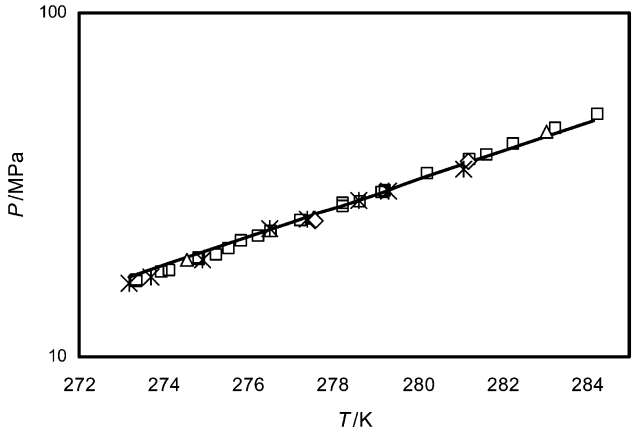

Figure 3. Measured and calculated dissociation conditions of nitrogen in the HLG region: —, calculated; □, van Cleeff and Diepen;[4,5] ◇, Marshal et al.;[6] ∗, Jhaveri and Robinson;[7] △, this work.

Table 5. Measured Oxygen Hydrate Dissociation Conditions in the HLG Region

T/K ± 0.2	P/kPa ± 34.47
273.80	13 558.25
276.55	17 563
279.05	23 284.07
284.55	43 755.86

Table 6. Binary Interaction Parameters for Oxygen−Water and Nitrogen−Water

oxygen−water	nitrogen−water
−0.357[a]	0.4792[a]
0.1424[b]	2.6575[b]
61.624[c]	64.46[c]

[a] k_{21} in non-density-dependent mixing rules.[19] [b] l^0_{21} in non-density-dependent mixing rules.[19] [c] $l^1_{21} \times 10^4$ in non-density-dependent mixing rules.[19]

For modeling air hydrates, it is necessary to measure experimental data and optimize the Kihara potential parameters for oxygen. To examine the reliability of the literature data, it was decided to measure four dissociation points on oxygen hydrates. These points are presented in Table 5.

The experimental data measured in this work, together with those reported in the literature in the HLG region, were employed in optimizing the Kihara potential parameters for oxygen. It should be noted that the modeling of a new hydrate forming compound consists of four steps: (1) modeling the phase behavior of the pure compound by introducing its physical constants; (2) calculating water−gas binary interaction parameters by using solubility data in water; (3) determining binary interaction parameters with other components; and (4) optimizing the Kihara potential parameters.

In this work, oxygen has been added to the thermodynamic model by introducing its physical constants and acentric factor. The binary interaction parameter between water and oxygen has been optimized by using oxygen solubility data,[30] but the binary interaction parameter between oxygen and other components has been set to zero. Table 6 presents the optimized binary interaction parameters for oxygen−water and also nitrogen−water.

The hard core radius, α, of the Kihara potential parameter for oxygen was calculated to be 0.2714 Å, from correlations given by Tee et al.[31] This value was considered acceptable for the hydrate modeling, as the results are not

Table 7. Kihara Potential Parameters for Nitrogen and Oxygen Assuming Structure I under Normal Conditions

compd	α/Å	σ^{*} [a]/Å	(ϵ/k)/K
nitrogen[b]	0.3350	3.2171	128.39
oxygen	0.2714	3.2701	133.074

[a] $\sigma^{*} = \sigma - 2\alpha$. [b] From ref 27.

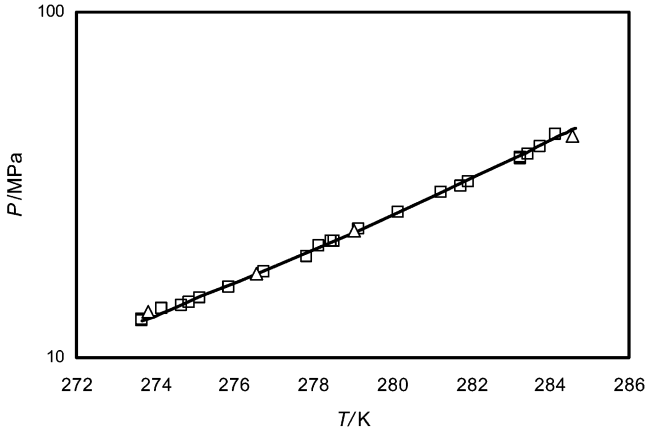

Figure 4. Measured and calculated dissociation conditions of oxygen hydrates in the HLG region: —, calculated; □, van Cleeff and Diepen;[5] △, this work.

Table 8. Measured Air Hydrate Dissociation Conditions in the HLG Region

T/K ± 0.2	P/kPa ± 34.47
274.05	17 004.68
276.35	21 126.61
278.65	26 489.25
280.45	32 361.96
283.55	45 113.75

significantly affected by minor changes in the core radius.[32,33] The other two Kihara potential parameters for oxygen, the collision diameter, σ, and the depth of the energy well, ϵ, were optimized by minimizing the absolute average deviation between the calculated and measured hydrate dissociation pressures of oxygen. Table 7 presents the optimized Kihara potential parameters for oxygen assuming structure I under the conditions investigated in this work. It is obvious that the Kihara potential parameters should only be used together with the reference parameters presented in Table 2. Figure 4 presents the hydrate dissociation data measured in this work, together with those reported in the literature, as well as the calculated values using the thermodynamic model described above.

Five dissociation points were then measured for hydrates formed from compressed air. As mentioned in Table 1, the air used was bottled synthetic from Air Products Ltd. with a reported composition of 18−21 mol % oxygen. Our calculations showed that the error due to the above variation in the concentration of oxygen is within the experimental error; therefore, no attempt was made to analyze the bottled air. The effect of other impurities (e.g., argon and carbon dioxide, as well as traces of neon, helium, and hydrogen) in the air was assumed to be negligible. Table 8 presents the measured hydrate dissociation points for air hydrates.

Figure 5 shows the experimental and predicted dissociation conditions for air hydrates in both HIG and HLG regions. An air composition of 21 mol % oxygen and 79 mol % nitrogen was assumed in running the thermodynamic model. As mentioned earlier, our results have shown that

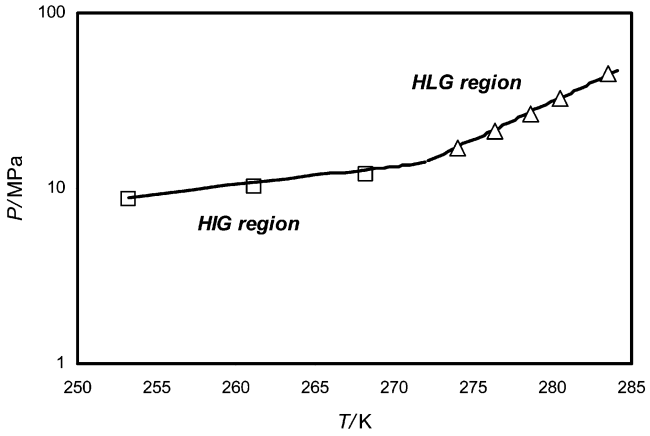

Figure 5. Measured and predicted dissociation conditions of air: —, prediction; □, Kuhs et al.;[3] △, this work.

air is likely to form structure I gas hydrates under the test conditions and structure II at low-temperature conditions. In this figure, assuming structure I for air hydrates gives better agreement with the experimental data reported in the HLG region. However, the thermodynamic model predicts a change in the stable hydrate structure with a reduction in the system temperature. The results show that predictions based on structure II hydrates are in better agreement with the three experimental data reported in the HIG region (Figure 5). Clearly, none of the air experimental data have been used in the optimization process. However, a final proof for the stable hydrate structure at various temperature conditions requires direct measurements by suitable physical techniques (e.g., NMR, X-ray, or Raman spectroscopy).

Conclusions

Air clathrate hydrates are stable at low-temperature and high-pressure conditions of deeper parts of ice sheets. Their role should be taken into account when conducting various studies on Arctic and Antarctic ice sheets. With the objective of measuring experimental data and developing a thermodynamic model for predicting the stability zone for air hydrates, a series of tests were conducted on methane, nitrogen, oxygen, and air hydrates.

A new experimental setup based on a quartz crystal microbalance (QCM) was used in measuring all the experimental data reported in this work. The new setup significantly reduces the quantity of sample, hence time, requirements for conducting the measurements.

Initially, the reliability of the experimental setup and techniques was examined and validated by measuring new experimental data on methane and nitrogen hydrates. Then, using the QCM setup, new experimental data were measured on oxygen hydrates and compared with the literature data. The available data on oxygen were employed in optimizing the Kihara potential parameters for this compound.

Finally, the QCM experimental setup was used to measure experimental data on air hydrates. The predictions of the thermodynamic model were compared with the independent data generated on air hydrates. Good agreement was achieved, demonstrating the reliability of the techniques used in this work.

Acknowledgment

The authors wish to thank Mr. Jim Pantling and Colin Flockhart for manufacture and maintenance of the experimental setup.

Nomenclature

HIG = hydrate−ice−gas region
HLG = hydrate−liquid water−gas region
k_{21} = binary interaction parameter for the conventional random mixing term
l_{21}^0 = dimensionless constant for the binary interaction parameter for the asymmetric term
l_{21}^1 = dimensionless constant for the binary interaction parameter for the asymmetric term
sI = structure I
QCM = quartz crystal microbalance
α = Kihara hard-core radius, Å
ΔC_{pw} = heat capacity difference between the empty hydrate lattice and liquid water, J mol^{-1}K^{-1}
ΔC_{pw}° = reference heat capacity difference between the empty hydrate lattice and liquid water at 273.15 K, J mol^{-1}K^{-1}
Δh_w° = enthalpy difference between the empty hydrate lattice and ice at the ice point and zero pressure, J mol^{-1}
Δv_w = molar volume difference between the empty hydrate lattice and ice, cm^3 mol^{-1}
$\Delta \mu_w^{\circ}$ = chemical potential difference between the empty hydrate lattice and ice at the ice point and zero pressure, J mol^{-1}
ϵ = Kihara energy parameter, J molecule^{-1}
k = Boltzmann's constant, J K^{-1} molecule^{-1}
σ = Kihara collision diameter, Å

Note Added after ASAP Posting. This article was released ASAP on 3/26/2003. In footnote *c* of Table 6, "$\times 10^4$" was added to l_{21}^1. The paper was reposted on 4/18/2003.

Literature Cited

(1) Sloan, E. D. *Clathrate hydrates of natural gases*, 2nd ed.; Marcel Dekker: New York, 1998.
(2) Anderson, R.; Tohidi, B.; Motaghi, S. Can gas hydrates solve the mysteries of Lake Vostok. *Proceedings of the fourth international conference on gas hydrates*, 19−23 May, 2002, Yokohama Symposia, Yokohama, Japan.
(3) Kuhs, W. F.; Klapproth, A.; Chazallon, B. Chemical physics of air clathrate hydrates. In *Physics of Ice Core Records*; Hondoh, T., Ed.; Hokkaido University, Press Sapporo: 2000; pp 373−393.
(4) van Cleeff, A.; Diepen, G. A. M. Gas hydrates of nitrogen and oxygen. *Recl. Trav. Chim.* **1960**, *84*, 1085−1093.
(5) van Cleeff, A.; Diepen, G. A. M. Gas hydrates of nitrogen and oxygen. II. *Recl. Trav. Chim.* **1965**, *84*, 1085−1093.
(6) Marshall, D. R.; Saito, S.; Kobayashi, R. Hydrates at high pressures: Part I. methane-water, argon-water and nitrogen-water systems. *AIChE J.* **1964**, *10* (2), 203.
(7) Jhaveri, J.; Robinson, D. B. Hydrates in the methane-nitrogen system. *Can. J. Chem. Eng.* **1965**, 75.
(8) Miller, S. L. Clathrate hydrates of air in Antarctic ice. *Science* **1969**, *165*, 489.
(9) Miller, S. L. The occurrence of gas hydrates in the solar system. *Proc. Natl. Acad. Sci. U.S.A.* **1961**, *47*, 1798−1808.
(10) Lipenkov, V. Y.; Istomin, V. A. On the stability of air clathrate-hydrate crystals in sub-glacial Lake Vostok, Antarctica. *Mater. Glyatsiol. Issled* **2001**, 91.
(11) Tohidi, B.; Danesh, A.; Todd, A. C.; Burgass, R. W. Application of quartz crystal microbalance gas hydrate stability zone measurement. *Proceedings of the fourth international conference on gas hydrates*, 19−23 May, 2002, Yokohama Symposia, Yokohama, Japan.
(12) Sauerbrey, G. Z. Investigation of Resonant Modes of Planoconvex AT-Plates. *Proceedings of the 21st Annual Freq. Control* **1967**, 63−71.
(13) Lu, C.; Czanderna, A. W. *Applications of piezoelectri quartz crystal microbalances*; Elsevier: Amsterdam, 1984; p 7.
(14) Burgass, R. W.; Todd, A. C.; Danesh, A.; Tohidi, B. Clathrate hydrate dissociation point detection and measurement. United States Patent number 6,298,724, 2001.
(15) Burgass, R. W.; Todd, A. C.; Danesh, A.; Tohidi, B. Dew Point and Bubble Point Measurement. United States Patent number 6,298,724, 2001.
(16) Avlonitis, D. Thermodynamics of gas hydrate equilibria. Ph.D. Thesis, Heriot-Watt University, 1992.
(17) Tohidi, B.; Burgass, R. W.; Danesh, A.; Todd, A. C. Hydrate inhibition effect of produced water, Part 1. Ethane and propane simple gas hydrates. *SPE 26701, Proceedings of the SPE Offshore Europe 93 Conference* **1993**, *1*, 255−264.
(18) Valderrama, J. O. A Generalized Patel-Teja equation of state for polar and nonpolar fluids and their mixtures. *J. Chem. Eng. Jpn.* **1990**, *23*, 87.
(19) Avlonitis, D.; Danesh, A.; Todd, A. C. Prediction of VL and VLL equilibria of mixtures containing petroleum reservoir fluids and methanol with a cubic EoS. *Fluid Phase Equilib.* **1994**, *94*, 181−216.
(20) van der Waals, J. H.; Platteeuw, J. C. Clathrate solutions. *Adv. Chem. Phys.* **1959**, *2*, 1−57.
(21) Parrish, W. R.; Prausnitz, J. M. Dissociation pressures of gas hydrates formed by gas mixtures. *Ind. Eng. Chem. Process Des. Dev.* **1972**, *11*, 26−35.
(22) Kihara, T. Virial coefficient and models of molecules in gases. *Rev. Mod. Phys.* **1953**, *25*, 831−843.
(23) Holder, G. D.; Cobin, G.; Papadopoulos, K. D. Thermodynamic and molecular properties of gas hydrates from mixtures containing methane, argon, and krypton. *Ind. Eng. Chem. Fundam.* **1980**, *19*, 282−286.
(24) Dharmawardhana, P. B.; Parrish, W. R.; Sloan, E. D. Experimental thermodynamic parameters for the prediction of natural gas hydrate dissociation conditions. *Ind. Eng. Chem. Fundam.* **1980**, *19*, 410−414.
(25) Davidson, D. W.; Handa, Y. P.; Ratcliffe, C. I.; Ripmeester, J. A.; Tse, J. S.; Dahn, J. R.; Lee, F.; Calvert, L. D. Crystallographic studies of clathrate hydrates. Part I. *Mol. Cryst. Liq. Cryst.* **1986**, *141*, 141−149.
(26) Tse, J. S.; Handa, Y. P.; Ratcliffe, C. I. Structure of oxygen clathrate hydrate by neutron powder diffraction. *J. Inclusion Phenom.* **1986**, *4*, 235−240.
(27) Tohidi-Kalorazi, B. Gas hydrate equilibria in the presence of electrolyte solutions. Ph.D. Thesis, Heriot-Watt University, 1995.
(28) Hendriks, E. M.; Edmonds, B.; Moorwood, R. A. S.; Szczepanski, R. Hydrate structure stability in simple and mixed hydrates. *Fluid Phase Equilib.* **1996**, *117*, 193−200.
(29) Hondoh, T.; Anzai, H.; Goto, A.; Mae, S.; Higashi, A.; Langway, C. C., Jr. The crystallographic structure of the natural air-hydrate in Greenland Dye-3 deep ice core, *J. Inclusion Phenom. Mol. Recognit. Chem.* **1990**, *8* (1/2), 17−24.
(30) Wilhelm, E.; Battino, R.; Wilcock, R. J. Low-pressure solubility of gases in liquid water. *Chem. Rev.* **1977**, *77* (2), 219.
(31) Tee, S. L.; Gotoh, S.; Stewart, W. E. Molecular parameters for normal fluids. *Ind. Eng. Chem. Fundam.* **1966**, *5*, 363−367.
(32) Holder, G. D.; Hand, J. H. Multiple-phase equilibria in hydrates from methane, ethane, propane and water mixtures. *AIChE J.* **1982**, *28*, 440−447.
(33) Mehta, A. P.; Sloan, E. D. A thermodynamic model for structure-H hydrates. *AIChE J.* **1994**, *40* (2), 312−320.

Received for review September 2, 2002. Accepted February 18, 2003. This work is supported by a Scottish Higher Education Funding Council (SHEFC) Research Development Grant, which is gratefully acknowledged.

JE025608X